Modelling of concrete at high temperatures: application to a PWR's vessel under LOCA load

Stefano Dal Pont[1)], Sabine Durand[2)], Bernhard Schrefler[3)]

1) BCC, LCPC, France (dalpont@lcpc.fr)
2) LM2S, CEA Saclay, France
3) DIC, University of Padova, Italy

ABSTRACT

The aim of this paper is to study the thermo-hydraulic behavior of concrete subjected to severe loading conditions, such as those typical of PWR's (Pressurized Water Reactors) vessels in accidental conditions. The paper presents a coupled Thermo-Hydro-Mechanical (THM) model for the description of concrete at high temperatures. The model is characterized by the presence of a deformable solid matrix (linearly elastic) filled with three fluid phases (liquid water, vapor water and dry air) and has been implemented in a finite element code (CAST3M) developed by the French research center for nuclear energy (CEA). The code has been validated by means of some simplified case-tests and by a comparison with a real scale structure submitted to high temperatures. Finally, the code has been applied for the prediction of the thermo-hydraulic conditions in a concrete slab submitted to a LOCA (Loss-of-Coolant Accident) load.

INTRODUCTION

Concrete is a porous material whose accurate description under thermal loading is important in the field of nuclear or civil engineering. Accidental scenarios considered for nuclear reactor containment buildings predict a rapid heating up to about *200°C*. Interim long-term storage structures are submitted to temperatures in the order of *80°C* over decades or centuries. These structures may also undergo accidents such as a ventilation stop which can increase temperature up to about *250°C* . The prediction of the response of concrete structures exposed to fire is another important field of application, [8], [5]. Many non-linear phenomena and interactions are involved in concrete behavior when high temperatures occur: the use of a fully coupled model is therefore necessary to correctly predict moisture migration and the magnitude of pore pressure [1]. A model has to take into account all the main phenomena that can be observed in porous media such as vapor diffusion, liquid water flow due to pressure gradients and capillary effects, evaporation/condensation phenomena,… Moreover, the porous structure of concrete experiences strong alterations. Temperature induces important changes in the pore structure due to the decomposition of hydrates, and the release of free water in the porous network. The consequence is that material characteristics entering the heat and mass transfer equations are strongly variable, e.g. permeability exhibits a sharp increase for temperatures above *105°C* [6]. The present model, deriving from the coupled formulation presented in [1], [8], [9] takes into account all the mentioned phenomena, typical of concrete at high temperatures.

THE MATHEMATICAL MODEL

We present in the following the main assumptions and hypothesis on which the full mathematical model is based. Porous media are usually analyzed from the macroscopic point of view accepting the continuum hypothesis of matter and then ignoring the discrete nature of the matter itself. This is the common approach used in thermodynamics. The underlying assumption is that at larger scales the macroscopic quantities of the constituents can be identified as statistical averages of molecular quantities. If the equations governing the system are written in local form, it is implied that the elementary volume considered is large enough so that the thermodynamic properties (that are averaged molecular properties) are meaningful. Moreover, a local thermodynamic equilibrium hypothesis must be assumed (local refers to the order of magnitude of the mean free path of the molecules). It is therefore necessary to establish that the timescale of the variations of the macroscopic system is much longer than the time required to reach equilibrium locally and that in the length scale considered there is a number of molecules large enough so that averaged molecular properties become meaningful. For the slow process considered here, the local thermodynamic assumption is usually accepted. Otherwise the continuum hypothesis must be abandoned and the thermodynamic quantities (pressure, temperature, etc) can not be defined. In such case the problem must be treated using a statistical thermodynamics approach. The porous medium poses additional problems because it is a heterogeneous system. To treat the porous medium as a system in which the properties are continuous functions of the space coordinates, some kind of larger scale volume averaging must be used (in addition to the statistical average at the molecular scale inside each phase, needed to define local thermodynamic properties). As proposed by several authors (mainly [2]) this can be done by introducing the concept of a Representative Elementary Volume (REV). The REV has obviously a length scale much greater than the molecular one previously mentioned and includes different components/phases. The definition of the REV allows us to introduce the set of governing differential equations at the macroscopic scale, by means of a procedure of spatial averaging on the REV of

the conservation equations written at the microscopic scale for the individual constituents of the medium (see [2]). This approach is not the only possible, but the reason for this choice is that averaging theories offer the possibility of a deep understanding of the microscopic situation and its relation to the macroscopic one. The full development of the averaging theory can be found in the original papers of Hassanizadeh and Gray [2], or more recently in [11]. The mathematical model consists of a series of equilibrium equations expressing the relationship existing between the thermodynamic coordinates and/or their variations at (thermodynamic) equilibrium. They then limit the number of independent coordinates needed to describe the state of the system. The appropriate (non-equilibrium) balance equations are the mass balance equation, the linear and angular momentum balance equation (for the fluid phases and the solid matrix) and the energy balance equation (given in the following in the final form).

Dry air balance equation

$$\phi\frac{\partial}{\partial t}[(1-S)\rho_{ga}] + (1-S)\rho_{ga}\frac{\partial\phi_{hydr}}{\partial t} + \alpha(1-S)\rho_{ga}\frac{\partial}{\partial t}(\nabla\cdot\mathbf{u}) + \nabla\cdot(\rho_{ga}\mathbf{v}_g) + \nabla\cdot(\rho_g\mathbf{v}^d_{ga}) = 0 \tag{1}$$

Water species (liquid-vapour) balance equation

$$\phi\frac{\partial}{\partial t}[(1-S)\rho_{gw}] + (1-S)\rho_{gw}\frac{\partial\phi_{hydr}}{\partial t} + \alpha(1-S)\rho_{gw}\frac{\partial}{\partial t}(\nabla\cdot\mathbf{u}) + \nabla\cdot(\rho_{gw}\mathbf{v}_g) + \nabla\cdot(\rho_g\mathbf{v}^d_{gw}) = -\phi\frac{\partial}{\partial t}(S\rho_w) - S\rho_w\frac{\partial\phi_{hydr}}{\partial t} - \alpha S\rho_w\frac{\partial}{\partial t}(\nabla\cdot\mathbf{u}) - \nabla\cdot[\rho_w\mathbf{v}_l] - \frac{\partial}{\partial t}(\Delta m_{hydr}) \tag{2}$$

Energy balance equation

$$\rho C_p\frac{\partial T}{\partial t} + [C_{pw}\rho_w\mathbf{v}_l + C_{pg}\rho_g\mathbf{v}_g]\nabla T - \nabla\cdot(\lambda_{eff}\nabla T) = \Delta h_{phase}\left[\phi\frac{\partial}{\partial t}(S\rho_w) + S\rho_w\frac{\partial\phi_{hydr}}{\partial t} + \alpha S\rho_w\frac{\partial}{\partial t}(\nabla\cdot\mathbf{u}) + \nabla\cdot(\rho_w\mathbf{v}_l)\right] + \Delta h_{hydr}\frac{\partial}{\partial t}(\Delta m_{hydr}) \tag{3}$$

Linear momentum conservation equation

$$\nabla\cdot\frac{\partial\sigma}{\partial t} + \frac{\partial\rho}{\partial t}\mathbf{b} = 0 \tag{4}$$

These balance equations are completed by an appropriate set of constitutive and state equations. These equations describe the specific behavior of the considered material, such as Fick's law of diffusion, Fourier's law for heat flux, Newton's law of viscosity or, again, other relations expressing the relative permeabilities or the effective diffusivity. These relationships are often obtained by exploitation of the entropy inequality: this procedure, leads to a consistent thermodynamic description of the material behavior at macro scale. The use of entropy inequality further assures that the second law of thermodynamics is not violated. This set of complementary equations is given in the annex. The governing equations of the model are given in terms of the chosen state variables. This choice is of particular importance: from a practical point of view, the chosen quantities should be easy to measure during experiments. From a theoretical point of view they must describe in a unique way the medium thermodynamic condition. Moreover they should guarantee a good numerical performance of the code. State variables have been determined in the number of five: gas pressure p_g, capillary pressure p_c, temperature T and displacement vector of the solid matrix $\boldsymbol{u}(u_x,u_y)$.

NUMERICAL SOLUTION

Discretization in time and in space of the governing equations is made by means of the finite element method. The classical notations of Zienkiewicz and Taylor [10] are adopted in the following together with vector notation. The unknown variables are expressed in terms of their nodal values as:

$$p_g(t) = \mathrm{N}_p \bar{\mathrm{p}}^g(t) \quad p_c(t) = \mathrm{N}_p \bar{\mathrm{p}}^c(t) \quad T(t) = \mathrm{N}_t \bar{\mathrm{T}} \quad \mathrm{u}(t) = \mathrm{N}_u \bar{\mathrm{u}} \tag{6}$$

The variational or weak form of equations is obtained in [7] by means of Galerkin's method (weighted residuals) and can be written in the following discretized matrix form:

$$\mathrm{C}_{ij}(\mathrm{x})\frac{\partial \mathrm{x}}{\partial t} + \mathrm{K}_{ij}(\mathrm{x})\mathrm{x} = \mathrm{f}_i(\mathrm{x}) \tag{7}$$

The time discretization is obtained by means of a fully implicit finite difference scheme (backward difference):

$$\psi^i(\mathrm{x}_{n+1}) = \mathrm{C}_{ij}(\mathrm{x}_{n+1})\frac{\mathrm{x}_{n+1} - \mathrm{x}_n}{\Delta t} + \mathrm{K}_{ij}(\mathrm{x}_{n+1})\mathrm{x}_{n+1} - \mathrm{f}_i(\mathrm{x}_{n+1}) = 0 \tag{8}$$

where *i=g,c,t,u* stands for the state variable, *n* is the time step number and Δt the time step length. The equation is solved by means of a Newton-Raphson iterative procedure.(see [9]).

The differential equations governing the problem have been finally solved introducing the system into CAST3M, a finite element code developed by the French research center for nuclear energy (CEA). The system has been solved following the scheme that follows, i.e. a partitioned procedure has been used.

- Input of material data/Mesh/time history
- Begin time loop
  - Begin TH+M loop
    - Begin TH loop
      - Loop on thermal equation
      - Loop on gas pressure equation
      - Loop on capillary pressure equation
    - End TH loop
    - Concatenated mechanics equation
  - End TH+M loop
- End time loop

This solution technique implies that within one time step every single equation is solved (via an iterative procedure requiring 2-5 cycles) for a given variable of the system while keeping the others constant. In particular, in the energy equation, T plays the role of the main variable, p_g is used in the dry air balance equation and p_c refers to the water species equation. This iterative procedure turns out to be an effective and relatively simple strategy to solve coupled problems. The global solution of the three equations describing the thermo-hydraulic behavior of the media, i.e. the final values of T, p_g and p_c, is found by means of an iterative procedure (TH loop) at every time step. Due to the elastic constitutive law, the dissipation due to plastic strain is neglected. The linear momentum balance equation then has not been included in the thermo-hydraulic (TH) loop but is linked with it through a thermo-hydraulic+mechanics loop (TH+M loop). It should be underlined that the sources of the CAST3M platform are freely available for research purposes: this means that the source code can be used and eventually adapted to specific user needs. This (nearly) unique feature is coupled with the fact that CAST3M is a finite element code developed by the French research center for nuclear energy, meaning that this code is naturally oriented to the solutions of common problems encountered in nuclear/civil engineering. Therefore, many mechanical constitutive laws (e.g. nonlocal damage, cohesive models, plasticity, …) are available and can be easily introduced in the proposed thermo-hydraulic coupled model. Moreover, the staggered procedure turns out to be a flexible way to solve the differential system of equations: every single equation can be replaced or adapted to specific uses as the general solution scheme does not change. In our opinion, this kind of approach contributes in an effective way to the advancement in the existing state of the art technology and has intrinsically many advantages compared to other similar existing codes such as e.g. the reference code in the field, Hitecosp [13].

NUMERICAL RESULTS

The presented procedure is validated by means of some test-cases. The numerical results are compared with a well-known code such as Hitecosp [13]. This code has been widely validated and can be considered as a reference in the study of the behavior of concrete at high temperature. The comparison and the validation of the model is based on the thermo-hydraulic answer of the system. In particular, results are given for the main variables of the system: the temperature T, the gas pressure p_g and the capillary pressure p_c. Given the main variables values, all the other fields can be calculated by means of the constitutive laws.

The analysis are performed on a concrete slab (see fig.1), meshed via 1x60 regular quadrangular 8-node elements.

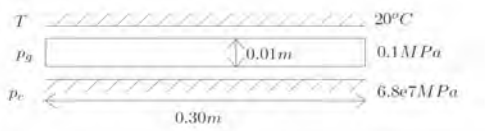

Figure 1. Slab scheme

Initial conditions, which are the same for all the test-cases, are given in fig.2.

Variable	Range	Unit
T	25	°C
p_g	0.1	MPa
p_c	6.8e7	MPa
u_x, u_y	0	m

Figure 2. Common initial conditions

Pure convection

This first example is characterized by the absence of diffusive phenomenon, i.e. transport phenomena are due only to convective effect. Temperature varies in the range *[298.15-358.15]K* with a velocity of *0.217K/s*. It should also be observed that in this first example, the temperature is limited to *85°C* (*358.15 K*), i.e. dehydration phenomena are neglected. This choice allows to further simplify the physical phenomena involved in the analysis and allows to verify the capacitive terms of the equations. Temperature, gas pressure and capillary pressure distribution on the slab at the final time step is given in fig.3. The correlation is very good, showing a good predictive capacity of our code: however, those aspects which have been neglected should be now introduced in the analysis.

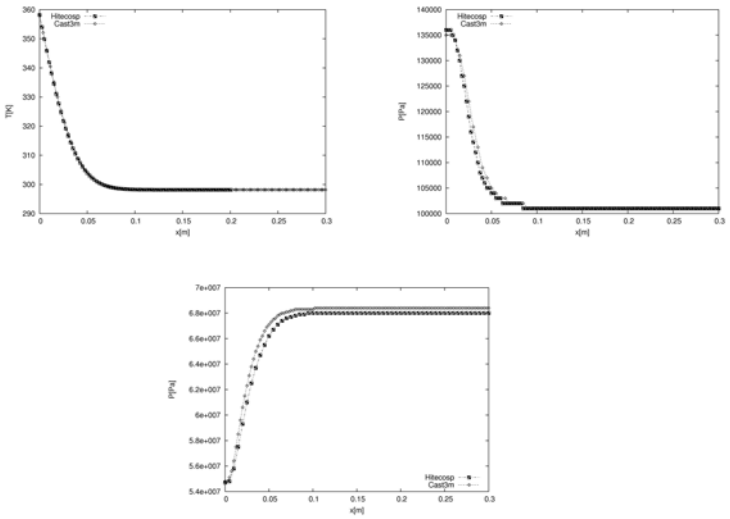

Figure 3. Comparison of temperature, gas pressure and capillary pressure

Capillary pressure gradient

In this case test, the slab is loaded by a capillary gradient on one side, i.e. a gradient of humidity on one of the sides of the slab is simulated. All transport phenomena are taken into account. Capillary pressure varies in the range *[6.8-3]x10^{7} MPa* with a velocity of *0.127 MPa/s*. This benchmark, involving a modest temperature gradient, is useful to verify the hydraulic phenomena. The correlation is satisfying, showing little discrepancies in the temperature and gas pressure maximal values. The distribution of these fields inside the slab shows a very good correspondence with the reference values. Temperature, gas pressure and capillary pressure distribution on the slab at the final time step is given in fig.4.

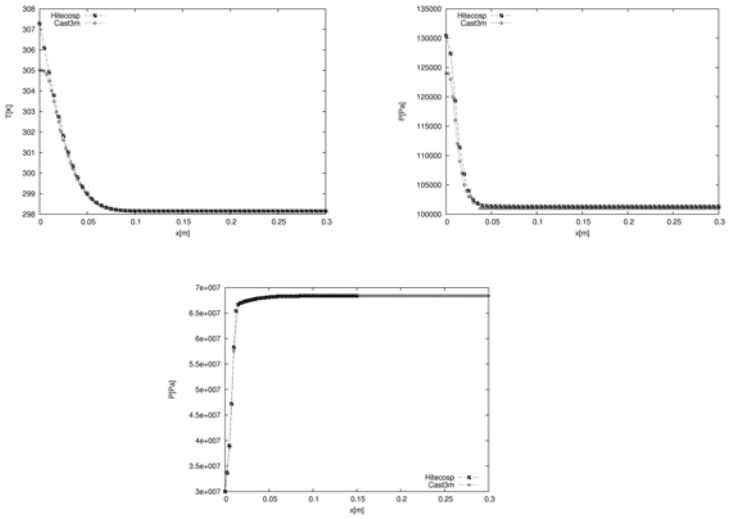

Figure 4. Comparison of temperature, gas pressure and capillary pressure

Temperature gradient

In this case test a Dirichlet-type condition on temperature is imposed in the range *[298.15-358.15]K* with a velocity of *0.217K/s*. As in the previous case, the temperature range is below the dehydration threshold in order to test more accurately the transport equations and to underline the (eventual) differences between the two models. Temperature, gas pressure and capillary pressure distribution on the slab at the final time step is given in fig.5. The comparison underlines a substantial coincidence of the results. However, small differences can be observed on gas and capillary pressure. These discrepancies were absent in the purely convective case, i.e. they have to be related to diffusive phenomena. The physical phenomena that can be observed in concrete at high temperature are concentrated in a few centimeters length, i.e. gradients are very strong and numerical instabilities can take place. This means that, given different ways of computing gradients (e.g. by means of a numerical vs. an analytical procedure), different results can be observed as a consequence of numerical artifices. In other words, small differences that can be observed while comparing numerical results issued from different numerical codes have to be expected.

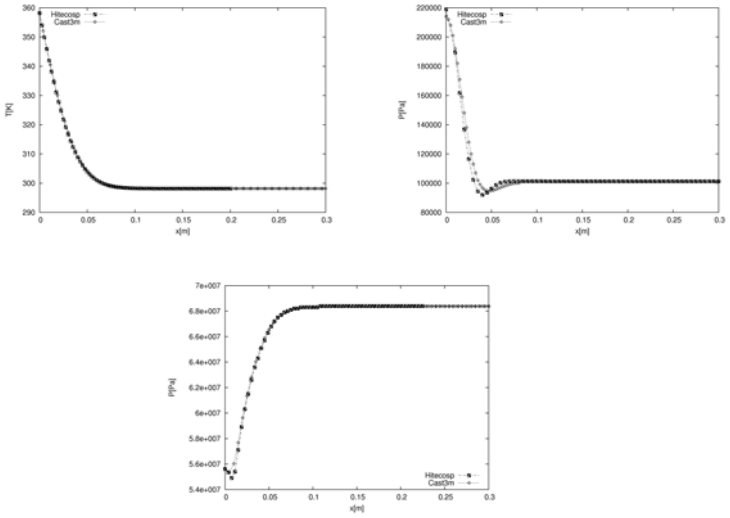

Figure 5. Comparison of temperature, gas pressure and capillary pressure

Heating of a hollow cylinder

In the following, the numerical code is validated by means of a comparison with an experimental set-up. The experiment has been performed on a hollow cylinder heated from the internal side, equipped with temperature and pressure sensors for the monitoring of the behavior of concrete. The cylinder is *1.5m* in height with an internal radius of *0.25m* and an external of *0.55m*. The cylinder dimensions have been chosen aiming at reproducing a real structure e.g. a wall of *30cm* of thickness. Full details about the experimental set-up are given in [12]. Concerning temperature measurements, a standard thermocouple of type K has been used. For what concerns the monitoring of gas pressures, the literature proposes a wide variety of sensors. Three sensors have been placed at *3, 16* and *25cm* from the heated surface. The cylinder has been heated on the internal face up to the temperature of *523.15K*, with a 5*K/h* velocity. Results are presented at time stations *t=20h, 40h, 60h*. Temperature profiles show a good correlation with experimental results (see fig.6a). The physical phenomena occurring inside the cylinder are characterized by a front of desaturation and a migration of water towards the colder zones. Desaturation is present in spite of the high water production that takes place when the temperature is above *378.15K* due to concrete dehydration; desaturation is caused by a rapid evaporation of water, resulting in formation of a zone of increased water vapour content. As expected the maximum peak of vapour pressure moves towards the external colder part of the cylinder (see fig.6b), following the free moisture migration (thermodiffusion). Concerning gas pressure, the comparison between experimental and numerical results on the pressure field underlines the predictive capacity of the code. The comparison on the first pressure sensor is only qualitative. Given the fact that during the ascending pressure phase, experimental gas pressure corresponds to saturating vapour pressure, it is reasonable to suppose that a small air sack on the gauge head produced a sort of "pressure cooker" effect, altering the experimental result. For what concerns the sensors at *16cm* and *25cm*, correlation is good, though, starting from about *t=170000s*, experimental pressures show an anomalous behaviour (which can be observed also on the pressure gauge at *3cm*); gas pressure dramatically decreases probably due to a macro-crack that formed on the line of the gauges and that let free moisture escape. Therefore, results should not be compared after this time.

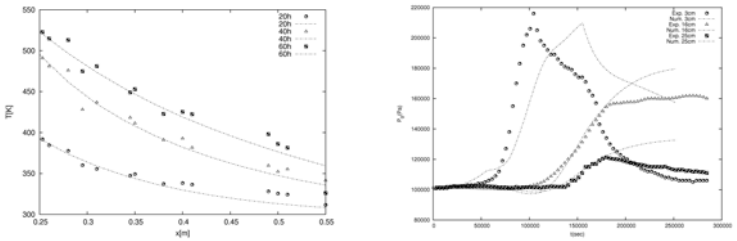

Figure 6. Comparison of temperatures and gas pressures

LOCA conditions

The examples presented in the previous section have allowed to substantially validate the presented model. As a case-test in this section a Loss-of-Coolant Accident (LOCA) condition is presented. This condition is a typical hypothetical accident in a nuclear reactor and provides an interesting load-case for our model applied to a realistic case. The PWR-LOCA accident load condition should be regarded as a pure numerical case-test in which important thermo-hydraulic gradients are involved and full range of temperatures, capillary and gas pressures are involved and investigated. The radial symmetry of a PWR's vessel can be exploited to simplify the study of the section, switching from a 3D problem to a 2D problem. The concrete slab is therefore submitted on one side to a thermal load (up to about 160°*C*, at a velocity of *22.5K/min* till *t=300s* and then *0.036K/min*: see fig.7) and to an hydraulic load (with a final pressure of about *0.8MPa*, velocity *65kPa/min* till *t=300s* and then *290Pa*: see fig.7).

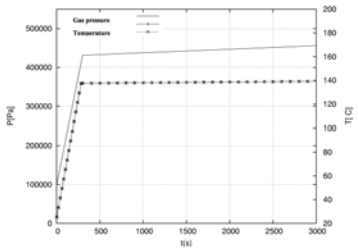

Figure 7. LOCA load condition

Results are given at the time stations *t=300s, 9000s, 27000s, 36000s*. Temperature profiles for the given time stations are given in fig.8. The comparison of the results shows a very good correlation with the reference code. As in the previous case, the correspondence between the results is satisfying, showing a good predictive capacity of the proposed model. The model has therefore allowed to describe the evolution of the thermo-hydraulic fields in concrete applied to nuclear power plants vessels allowing to obtain a reliable prediction of the behavior of concrete.

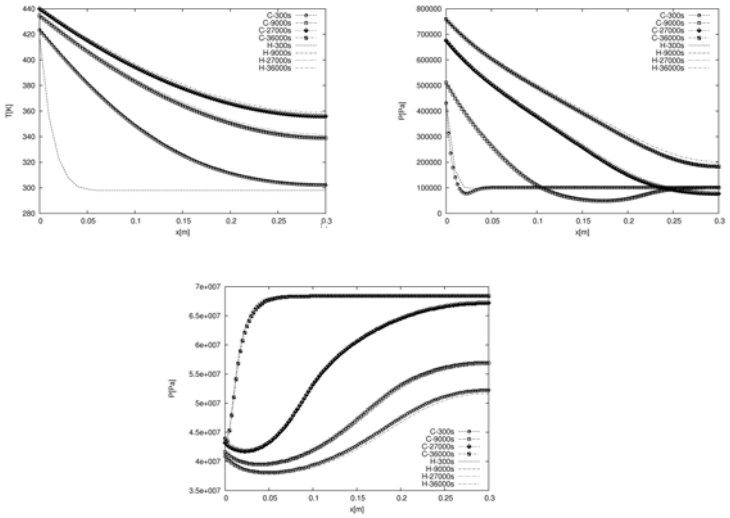

Figure 8. Comparison of temperatures and gas pressures

CONCLUSION

This paper has presented a coupled thermo-hydro-mechanical model for the description of the behavior of concrete at high temperatures. The mathematical model is mainly characterized by three fluid phases and a deformable solid matrix and has been implemented in a finite element code developed by the French research center for nuclear energy (CEA). The code has been then validated by means of some representative cases and has been finally compared to an experimental set-up and applied to a concrete slab (representative of a nuclear power plant vessel) submitted to LOCA conditions. This analysis has allowed to predict the distribution of the thermo-hydraulic fields inside concrete, showing a substantial coincidence with the reference results.

REFERENCES

1. Lewis, R.W. and Schrefler, B.A.. (1998). "The Finite Element Method in the static and dynamic deformation and consolidation of porous media" ed: J.Wiley&Sons.
2. Gray,W.G. and Hassanizadeh,S.M.. (1979). "General conservation equations for multiphase systems: 2. mass, momenta, energy and entropy transfer", Adv.Water.Res,, 2, 191-203
3. Gawin, D. and Schrefler, B.A. and Pesavento, F.(2002), "Modelling of hygro-thermal behavior and damage of concrete at temperature above the critical point of water" Int.J.Numer.Anal.Meth.Geomech, 26, 537-562
4. Dal Pont, S. and Ehrlacher, A.(2004) "Numerical and experimental analysis of chemical dehydration, heat and mass transfer in a concrete hollow cylinder submitted to high temperatures", Int.J.Heat and Mass transfer, 1, 4, 135-147
5. Ulm, F.J. and Coussy, O. and Bazant, Z. (1999), "The "Chunnel" fire. II: analysis of concrete damage" J.Eng.Mech., 3, 283-289
6. Bazant, Z.P. and Whittmann, F.H.(1982), "Creep and shrinkage in concrete structures", J.Wiley&Sons
7. Pesavento,F. (2000), "Non linear modelling of concrete as multiphase material in high temperature conditions", Ph.D. thesis, Università degli Studi di Padova, Italy
8. Gawin, D. and Schrefler, B.A. and Pesavento, F.(2002),"Modelling of hygro-thermal behavior and damage of concrete at temperature above the critical point of water", Int.J.Numer.Anal.Meth.Geom., 26, 537-562
9. Gawin, D. and Pesavento, F. and Schrefler, B.A.(2003),"Modelling of hygro-thermal behaviour of concrete at high temperature with thermo-chemical and mechanical material degradation", Comput.Methods Appl.Mech.Engrg., K476, vol.K3, 192, 1731-1771
10. Taylor, R.L. amd Zienkiewicz, O.C. (1988), "The finite element method", McGraw-Hill
11. Schrefler, B.A.,(2002), "Mechanics and thermodynamics of saturated/unsaturated porous materials and quantitative solutions", Appl.Mech.Rev., 4, 351-388
12. Dal Pont, S.(2004), "Lien entre la perméabilité et l'endommagement dans les bétons à haute température" Ph.D. thesis, ENPC,Paris
13. Brite Euram III BRPR-CT95-0065 Hiteco, Understanding and industrial application of high performance concrete in high temperature environment-Final Report, 1999